Delamination behaviour of composites

Related titles:

Multi-scale modelling of composite material systems
(ISBN 978-1-85573-936-9)
Predictive modelling provides the opportunity both to understand better how composites behave in different conditions and to develop materials with enhanced performance for particular industrial applications. This important book focuses on the fundamental understanding of composite materials at the microscopic scale, from designing micro-structural features, to the predictive equations of the functional behaviour of the structure for a specific end-application. Chapters discuss stress and temperature-related behavioural phenomena based on knowledge of physics of microstructure and microstructural change over time.

Impact behaviour of fibre-reinforced composite materials and structures
(ISBN 978-978-1-8573-423-4)
This study covers impact response, damage tolerance and failure of fibre-reinforced composite materials and structures. Materials development, analysis and prediction of structural behaviour and cost-effective design all have a bearing on the impact response of composites and this book brings together for the first time the most comprehensive and up-to-date research work from leading international experts.

Mechanical testing of advanced fibre composites
(ISBN 978-1-85573-312-1)
Testing of composite materials can present complex problems but is essential in order to ensure the reliable, safe and cost-effective performance of any engineering structure. *Mechanical testing of advanced fibre composites* describes a wide range of test methods which can be applied to various types of advanced fibre composites. The book focuses on high modulus, high strength fibre/plastic composites and also covers highly anisotropic materials such as carbon, aramid and glass.

Details of these and other Woodhead Publishing materials books, as well as materials books from Maney Publishing, can be obtained by:

- visiting our web site at www.woodheadpublishing.com
- contacting Customer Services (e-mail: sales@woodhead-publishing.com; fax: +44 (0) 1223 893694; tel: +44 (0) 1223 891358 ext: 130; address: Woodhead Publishing Ltd, Abington Hall, Granta Park, Great Abington, Cambridge CB21 6AH, England)

If you would like to receive information on forthcoming titles, please send your address details to: Francis Dodds (address, tel. and fax as above; e-mail: francisd@woodhead-publishing.com). Please confirm which subject areas you are interested in.

Maney currently publishes 16 peer-reviewed materials science and engineering journals. For further information visit www.maney.co.uk/journals

Delamination behaviour of composites

Edited by
Srinivasan Sridharan

Published by Woodhead Publishing and Maney Publishing
on behalf of
The Institute of Materials, Minerals & Mining

CRC Press
Boca Raton Boston New York Washington, DC

WOODHEAD PUBLISHING LIMITED
Cambridge England

Woodhead Publishing Limited and Maney Publishing Limited on behalf of
The Institute of Materials, Minerals & Mining

Woodhead Publishing Limited, Abington Hall, Granta Park, Great Abington, Cambridge CB21 6AH, England
www.woodheadpublishing.com

Published in North America by CRC Press LLC, 6000 Broken Sound Parkway, NW, Suite 300, Boca Raton, FL 33487, USA

First published 2008, Woodhead Publishing Limited and CRC Press LLC

British Library Cataloguing in Publication Data
A catalogue record for this book is available from the British Library.

Library of Congress Cataloging in Publication Data
A catalog record for this book is available from the Library of Congress.

Woodhead Publishing ISBN 978-1-84569-244-5 (book)
Woodhead Publishing ISBN 978-1-84569-482-1 (e-book)
CRC Press ISBN 978-1-4200-7967-8
CRC Press order number: WP7967

The publishers' policy is to use permanent paper from mills that operate a sustainable forestry policy, and which has been manufactured from pulp which is processed using acid-free and elementary chlorine-free practices. Furthermore, the publishers ensure that the text paper and cover board used have met acceptable environmental accreditation standards.

Project managed by Macfarlane Book Production Services, Dunstable, Bedfordshire, England (e-mail: macfarl@aol.com)
Typeset by Replika Press Pvt Ltd, India
Printed by T J International Limited, Padstow, Cornwall, England

Contents

Contributor contact details

(* = main contact)

Introduction

S. Sridharan*
Department of Mechanical, Aerospace and Structural Engineering
Washington University in St. Louis
St. Louis, MO 63130
USA

E-mail: ssrid@seas.wustl.edu

Chapter 1

I. S. Raju* and T. K. O'Brien
NASA-Langley Research Center Hampton, VA 23861
USA

E-mail: ivatury.s.raju@nasa.gov

Chapter 2

A. Riccio
C I R A (Centro Italiano Ricerche Aerospaziali – Italian Aerospace Research Centre)
Via Maiorise, S/N
81043
Capua (Caserta)
Italy

E-mail: a.riccio@cira.it

Chapter 3

P. Davies
Materials and Structures Group
(DOP/DCB/ERT/MS)
IFREMER Centre de Brest
BP70
29280 Plouzané
France

E-mail: peter.davies@ifremer.fr

Chapter 4

C. Sun
School of Aeronautics and Astronautics
Purdue University
West Lafayette, IN 47907
USA

E-mail: sun@purdue.edu

Chapter 5

R. Ganesan
Concordia Centre for Composites
Department of Mechanical and Industrial Engineering
Concordia University
Room EV 4 - 211, 1515 St Catherine West
Montreal
Quebec H3G 2W1
Canada

E-mail: ganesan@encs.concordia.ca

Chapter 6

P. Tan?[1] and L. Tong*
School of Aerospace
Mechanical and Mechatronic Engineering
University of Sydney
NSW 2006
Australia

E-mail: ltong@aeromech.usyd.edu.au
pingtan@aeromech.usyd.edu.au

Chapter 7

Z. Su
The Department of Mechanical Engineering
The Hong Kong Polytechnic University
Hung Hom
Kowloon
Hong Kong

E-mail: mmsu@polyu.edu.hk
szq@aeromech.usyd.edu.au;

L. Ye*
Centre for Advanced Materials Technology (CAMT)
School of Aerospace
Mechanical and Mechatronic Engineering (AMME)
The University of Sydney
NSW 2006
Australia

E-mail: ye@aeromech.usyd.edu.au

Chapter 8

J. Bohse*
BAM – Federal Institute for Materials Research and Testing
Division V.6 Mechanical Behaviour of Polymers
Unter den Eichen 87
D-12205 Berlin
Germany

E-mail: juergen.bohse@bam.de

A. J. Brunner
Laboratory for Mechanical Systems Engineering
Empa – Swiss Federal Laboratories for Materials Testing and Research
Ueberlandstrasse 129
CH-8600 Duebendorf
Switzerland

E-mail: andreas.brunner@empa.ch

[1] Ping Tan is currently working as a research scientist at the Australian Defence Science and Technology Organisation

Chapter 9

A. J. Brunner
Laboratory for Mechanical Systems Engineering
Empa – Swiss Federal Laboratories for Materials Testing and Research
Ueberlandstrasse 129
CH-8600 Duebendorf
Switzerland

E-mail: andreas.brunner@empa.ch

Chapters 10 and 11

Marcelo Francisco de Sousa Ferreira de Moura
Departamento de Engenharia Mecânica e Gestão Industrial
Faculdade de Engenharia da Universidade do Porto
Rua Dr. Roberto Frias s/n, 4200-465 Porto
Portugal

E-mail: mfmoura@fe.up.pt

Chapter 12

F. Avilés*
Centro de Investigación Científica de Yucatán, A.C.
Unidad de Materiales
Calle 43 # 103
Col. Chuburná de Hidalgo
C.P. 97200.
Mérida
Yucatán
México

L. Carlsson
Department of Mechanical Engineering
Florida Atlantic University
Boca Raton, FL 33431
USA

E-mail: faviles@cicy.mx
carlsson@fau.edu

Chapter 13

S. Hallett
Advance Composites Centre for Innovation and Science
University of Bristol
Queens Building
University Walk
Bristol BS8 1TR
UK

E-mail: Stephen.Hallett@bristol.ac.uk

Chapters 14 and 21

S. Sridharan*
Department of Mechanical, Aerospace and Structural Engineering
Washington University in St. Louis
St. Louis, MO 63130
USA

E-mail : ssrid@seas.wustl.edu

Y. Li
Intel Corporation
Chandler, AZ 85224
USA

E-mail: yupeng.lizzy.li@intel.com

Chapter 15

R. Yu*
E.T.S Ingenieros de Caminos, Canales y Puertos
Universidad de Castilla-La Mancha
13071 Ciudad Real
Spain

E-mail: rena@uclm.es

A. Pandolfi
Dipartimento di Ingegneria Strutturale
Politecnico di Milano
Piazza Leonardo da Vinci 32
20133 Milano
Italy

E-mail: pandolfi@stru.polimi.it

Chapter 16

B. Blackman
Department of Mechanical Engineering
Imperial College London
London SW7 2AZ
UK

E-mail: b.blackman@imperial.ac.uk

Chapter 17

P. Camanho*
DEMEGI
Faculdade de Engenharia
Universidade do Porto
Rua Dr. Roberto Frias
4200-465 Porto
Portugal

E-mail: pcamanho@fe.up.pt

A. Turon and J. Costa
AMADE
Polytechnic School
University of Girona
Campus Montilivii s/n
17071 Girona
Spain

Chapter 18

Roberta Massabò
Department of Civil, Environmental and Architectural Engineering
University of Genova
Via Montallegro, 1
16145, Genova
Italy

E-mail: roberta.massabo@unige.it

Chapter 19

Alastair F. Johnson and Nathalie Toso-Pentecôte
German Aerospace Center (DLR)
Institute of Structures and Design
Pfaffenwaldring 38-40
70569 Stuttgart
Germany

E-mail: alastair.johnson@dlr.de

Chapter 20

A. Tafreshi
School of Mechanical
Aerospace and Civil Engineering
The University of Manchester
P.O. Box 88
Sackville Street
Manchester M60 1QD
UK

E-mail:
azam.tafreshi@manchester.ac.uk

Chapter 22

M. Kessler
Iowa State University
Materials Science and Engineering
2220 Hoover Hall
Ames, IA 50011-2300
USA
E-mail: mkessler@iastate.edu

Chapter 23

H. Liu*
Centre for Advanced Materials
Technology
School of Aerospace
Mechanical and Mechatronic
Engineering
The University of Sydney
Sydney
NSW 2006
Australia

E-mail: hong-yuan.liu@usyd.edu.au

W. Yan
Department of Mechanical
Engineering
Monash University
Melbourne
Victoria 3800
Australia

E-mail:
wenyi.yan@eng.monash.edu.au

Chapter 24

M. R. Wisnom
University of Bristol
Advanced Composites Centre for
Innovation and Science
Queens Building
University Walk
Bristol BS8 1TR
UK

E-mail: M. Wisnom@bristol.ac.uk

Chapter 25

S. Mall
Air Force Institute of Technology
AFIT/ENY
Bldg. 640
2950 Hobson Way
Wright-Patterson AFB, OH 45433
USA

E-mail: shankar.mall@afit.edu

Introduction

S SRIDHARAN, Washington University in St. Louis, USA

Laminated composites are becoming the preferred material system in a variety of industrial applications, such as aeronautical and aerospace structures, ship hulls in naval engineering, automotive structural parts, micro-electro-mechanical systems as also civil structures for strengthening concrete members. The increased strength and stiffness for a given weight, increased toughness, increased mechanical damping, increased chemical and corrosion resistance in comparison to conventional metallic materials and potential for structural tailoring are some of the factors that have contributed to the advancement of laminated composites. Their increased use has underlined the need for understanding their modes of failure and evolving technologies for the continual enhancement of their performance.

The principal mode of failure of layered composites is the separation along the interfaces of the layers, *viz*. delamination. This type of failure is induced by interlaminar tension and shear that develop due to a variety of factors such as: Free edge effects, structural discontinuities, localized disturbances during manufacture and in working condition, such as impact of falling objects, drilling during manufacture, moisture and temperature variations and internal failure mechanisms such as matrix cracking. Hidden from superficial visual inspection, delamination lies often buried between the layers, and can begin to grow in response to an appropriate mode of loading, drastically reducing the stiffness of the structure and thus the life of the structure. The delamination growth often occurs in conjunction with other modes of failure, particularly matrix cracking.

A study of composite delamination, as does any technological discipline, has two complementary aspects: An in depth understanding of the phenomenon by analysis and experimentation and the development of strategies for effectively dealing with the problem. These in turn lead to a number of specific topics that we need to consider in the present context. These comprise of:

1. An understanding of the basic principles that govern the initiation of delamination, its growth and its potential interaction with other modes of failure of composites. This is the theme of the first chapter, but several authors return to this theme in their own respective contributions.
2. The determination of material parameters that govern delamination initiation and growth by appropriate testing. These must necessarily be interfacial strength parameters which govern interlaminar fracture initiation and interlaminar fracture toughness parameters, *viz*. critical strain energy release rates that must govern interlaminar crack growth. The book contains several valuable contributions from leading international authorities in the field of testing of composites.
3. Development of analytical tools : What are the methodologies one may employ to assess the possibility of delamination onset and growth under

typical loading scenarios? This may be approached from the points of view of fracture mechanics, damage mechanics, cohesive modeling approach and approaches which draw from and combine these. In particular, the cohesive modeling approach has proven to be a powerful and versatile tool in that when embedded in a nonlinear finite element analysis, it can trace the two-dimensional delamination growth without user interference, is robust from the point of view of numerical convergence, and can potentially account for a variety of interfacial failure mechanisms. This subject is discussed thoroughly in several authoritative contributions.

4. Detection of delamination: Ability to diagnose the presence of delamination and to be able to capture in graphical terms the extent of delamination damage is a desideratum towards which the composite industry is continuing to make progress. Several nondestructive evaluation tools are available and have been used with varying degrees of success. Acoustic emission, Lamb-wave and Piezo-electric technologies are discussed in the context of delamination detection in the present work.
5. Prevention of delamination: Several techniques of either inhibiting delamination or altogether suppressing it are available. The book contains a section treating the following techniques of delamination prevention/inhibition: 'Self-healing' composites which internally exude adhesive material as soon as crack advances thus effectively arresting the crack; Z-pin bridging in which fibers are introduced across the interlaminar surfaces, liable to delaminate, artfully tapering off discontinuities which are sources of potential delamination and the use of toughened epoxies.
6. Delamination driven structural failure: Certain loading scenarios can cause delamination growth if there is some preexisting delamination in the structural component which in turn can lead to structural failure. Typically these are: Impact, cyclic loading (delamination due to fatigue), compressive loading causing localized buckling in the vicinity of delamination and dynamic loading in the presence of in-plane compression. Impact loading and any form of dynamic loading in the presence of significant compressive stress in sandwich structures are known to trigger delamination failure which is abrupt and total. These aspects have been discussed in several contributions.

The book has been divided into several sections to address the issues mentioned in the foregoing. It has been a pleasure to work with a number of authors of international standing and reputation who had spent a great deal of effort in developing their respective chapters. The references cited at the end of each chapter should supplement and corroborate the concepts developed in the chapter. We hope that researchers and engineers who are concerned to apply state of the art technologies to composite structural analysis, design and evaluation of risk of failure will find this book useful and a valuable source of insight.

10
Interlaminar mode II fracture characterization

M. F. S. F. de MOURA, Faculdade de Engenharia da Universidade do Porto, Portugal

10.1 Introduction

The application of composite materials in the aircraft and automobile industries has led to an increase of research into the fracture behaviour of composites. One of the most significant mechanical properties of fibre reinforced polymer composites is its resistance to delamination onset and propagation. It is known that delamination can induce significant stiffness reduction leading to premature failures. Delamination can be viewed as a crack propagation phenomenon, thus justifying a typical application of fracture mechanics concepts. In this context, the interlaminar fracture characterization of composites acquires remarkable relevancy. There are several tests proposed in the literature in order to measure the interlaminar strain energies release rates in mode I, mode II and mixed mode I/II. Whilst mode I has already been extensively studied and the Double Cantilever Test (DCB) test is universally accepted, mode II is not so well studied, which can be explained by some difficulties inherent to experimental tests. Moreover, in many real situations delaminations propagate predominantly in mode II, as is the case of composite plates under low velocity impact (Choi and Chang, 1992). This gives relevancy to the determination of toughness propagation values instead of the initiation ones commonly considered in design. Some non-negligible differences can be achieved considering the *R*-curve effects (de Morais and Pereira, 2007). These issues make the fracture characterization in mode II an actual and fundamental research topic. However, problems related to unstable crack growth and to crack monitoring during propagation preclude a rigorous measurement of G_{IIc}. In fact, in the mode II fracture characterization tests the crack tends to close due to the applied load, which hinders a clear visualization of its tip. In addition, the classical data reduction schemes, based on beam theory analysis and compliance calibration, require crack monitoring during propagation. On the other hand, a quite extensive Fracture Process Zone (FPZ) ahead of crack tip exists under mode II loading. This non-negligible FPZ affects the measured toughness as a non-negligible amount of energy is dissipated on it. Consequently, its influence should be taken into account, which does not occur when the real crack length is used in the selected data reduction scheme. To overcome these difficulties a new data reduction scheme based on crack equivalent concepts and depending only on the specimen compliance is presented in the next section. The main objective of the proposed methodology is to increase the accuracy of experimental mode II fracture tests on the G_{IIc} measurements. In fact, a rigorous monitoring of the crack length during propagation is one of the complexities of these tests.

10.2 Static mode II fracture characterization

There are three fundamental experimental tests used to measure G_{IIc}. The most popular one is the End Notched Flexure (ENF), which was developed for wood fracture characterization (Barrett and Foschi, 1977). The test consists on a pre-cracked specimen under three point bending loading (see Fig. 10.1).

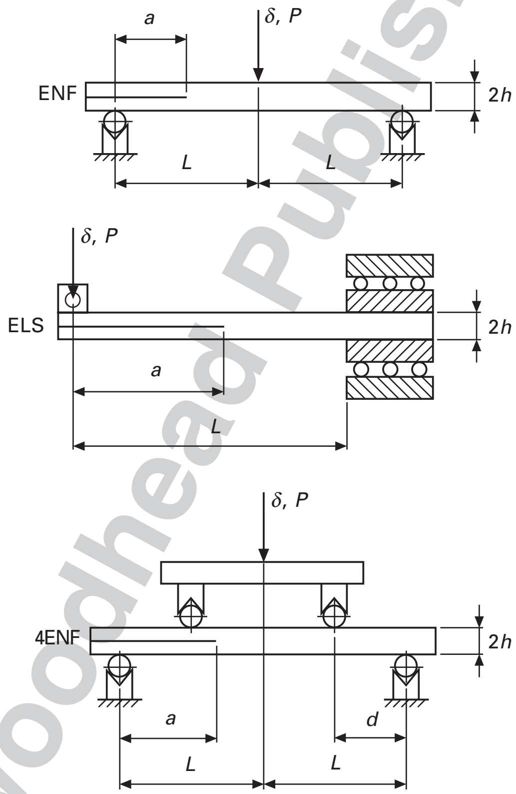

10.1 Schematic representations of the mode II tests.

Unstable crack propagation constitutes one of the disadvantages of the ENF test. Another possibility is the End Loaded Split (ELS) test which is based on cantilever beam geometry (see Fig. 10.1). Although the ELS test involves more complexities during experiments relatively to the ENF test, it provides a larger range of crack length where the crack propagates stably. In fact, the ENF test requires $a_0/L>0.7$ to obtain stable crack propagation (Carlsson *et al*., 1986), whereas in the ELS test $a_0/L>0.55$ is sufficient (Wang and Vu-Khanh, 1996). However, both of these tests present a common difficulty related to the crack length measurement during the experimental test. Different methods have been proposed in literature to address these difficulties. Kageyama *et al*. (1991) proposed a Stabilized End Notched Flexure (SENF) test for experimental characterization of mode II crack growth. A special displacement gage was developed for direct measurement of the relative shear slip between crack surfaces of the ENF specimen. The test was performed under constant crack shear displacement rate, which guarantees stable crack propagation. Yoshihara *et al*. (Yoshihara and Ohta, 2000) recommended the use of Crack Shear Displacement method (CSD) to obtain the mode II *R*-curve since the crack length is implicitly included in the CSD. Tanaka *et al.* (Tanaka *et al*., 1995) concluded that to extend the stabilized crack propagation range in the ENF test, the test should be done under a condition of controlled CSD. Although the CSD method provides the measurement of the mode II toughness without crack length monitoring, this method requires a servo valve-controlled testing machine and the testing procedure is more complicated than that under the loading point displacement condition. Alternatively the Four Point End Notched Flexure test (4ENF) (Fig. 10.1) can be used to evaluate the mode II *R*-curve. This test does not require crack monitoring but involves a more sophisticated setup and larger friction effects were observed (Shuecker and Davidson, 2000). In the following, a summary of the classical reduction schemes used for these experimental tests is presented.

10.2.1 Classical methods

Compliance calibration method (CCM)

The CCM is the most used. During the test the values of load, applied displacement and crack length (P-δ-a) are registered in order to calculate the critical strain energy release rate using the Irwin-Kies equation (Kanninen and Popelar, 1985)

$$G_{\mathrm{IIc}} = \frac{P^2}{2B}\frac{dC}{da} \qquad 10.1$$

where B is the specimen width and $C = \delta/P$ the compliance. In the ENF and ELS tests a cubic relationship between the compliance (C) and the measured crack length a is usually assumed (Davies *et al*., 2001)

$$C = D + ma^3 \qquad 10.2$$

where D and m are constants. G_{IIc} is then obtained from

$$G_{IIc} = \frac{3P^2 m a^2}{2B} \qquad 10.3$$

For the 4ENF test a linear relationship (Yoshihara, 2004) between the compliance (C) and the measured crack length a is used

$$C = D + ma \qquad 10.4$$

being D and m the respective coefficients. It should be noted that relations $C = f(a)$ given by Equations 10.2 and 10.4 are based on the beam theory approach, as it will be shown in the next sub-section. G_{IIc} is given by

$$G_{IIc} = \frac{P^2}{2B} m \qquad 10.5$$

The three tests require the calibration of the compliance in function of the crack length. This can be done by measurement of crack length during propagation or, alternatively, considering several specimens with different initial cracks lengths to establish the compliance–crack length relation, which is regressed by cubic (Equation 10.2) and linear (Equation 10.4) functions.

Beam theory

Beam theory methods are also frequently used to obtain G_{IIc} in mode II tests. In the case of ENF test Wang and Williams (1992) proposed the Corrected Beam Theory (CBT)

$$G_{IIc} = \frac{9(a + 0.42\Delta_I)^2 P^2}{16B^2 h^3 E_1} \qquad 10.6$$

where E_1 is the axial modulus and Δ_I a crack length correction to account for shear deformation

$$\Delta_I = h\sqrt{\frac{E_1}{11G_{13}}\left[3 - 2\left(\frac{\Gamma}{1 + \Gamma}\right)^2\right]} \qquad 10.7$$

with

$$\Gamma = 1.18\frac{\sqrt{E_1 E_2}}{G_{13}} \qquad 10.8$$

where E_2 and G_{13} are the transverse and shear moduli, respectively. In the ELS case a similar expression is proposed (Wang and Williams, 1992)

$$G_{IIc} = \frac{9(a + 0.49\Delta_I)^2 P^2}{4B^2 h^3 E_1} \qquad 10.9$$

For the 4ENF test the beam theory leads to the following equation (Silva, 2006)

$$C = \frac{d}{24\,E_1 I}\,(18\,d\,a - 20\,d^2 + 60\,L^2 - 6\,d\,L) \qquad 10.10$$

where I is the second moment of area and d represents the distance between each support and its nearest loading actuator (Fig. 10.1). Using Equation [10.1] G_{IIc} can be obtained from

$$G_{\mathrm{IIc}} = \frac{9}{16}\,\frac{P^2 d^2}{E_1 B^2 h^3} \qquad 10.11$$

In summary, the application of beam theory to ENF and ELS tests involves the crack length, which does not occur in the 4ENF test. However, it should be emphasized that 4ENF setup is more complex. Also, friction effects (Shuecker and Davidson, 2000) and system compliance (Davidson and Sun, 2005) can affect the results. Owing to these drawbacks of the 4ENF test, the ENF and ELS tests emerge as the most appropriate to fracture characterization of composites in mode II. In this context, a new data reduction scheme, not depending on the crack length measurements, is proposed in the following section for these experimental tests.

10.2.2 Compliance based beam method (CBBM)

In order to overcome the difficulties associated to classical data reduction schemes a new method is proposed. The method is based on crack equivalent concept and depends only on the specimen compliance. The application of the method to ENF and ELS tests is described in the following.

ENF test

Following strength of materials analysis, the strain energy of the specimen due to bending and including shear effects is

$$U = \int_0^{2L} \frac{M_f^2}{2\,E_f I}\,dx + \int_0^{2L}\int_{-h}^{h} \frac{\tau^2}{2\,G_{13}}\,B\,dy\,dx \qquad 10.12$$

where M_f is the bending moment and

$$\tau = \frac{3}{2}\,\frac{V_i}{A_i}\left(1 - \frac{y^2}{c_i^2}\right) \qquad 10.13$$

where A_i, c_i and V_i represent, respectively, the cross-section area, half-thickness of the beam and the transverse load of the i segment ($0 \le x \le a$, $a \le x \le L$ or

$L \leq x \leq 2L$). From the Castigliano theorem, the displacement at the loading point for a crack length a is

$$\delta = \frac{dU}{dP} = \frac{P(3a^3 + 2L^3)}{8E_f Bh^3} + \frac{3PL}{10G_{13}Bh} \qquad 10.14$$

Since the flexural modulus of the specimen plays a fundamental role on the P-δ relationship, it can be calculated from Equation 10.14 using the initial compliance C_0 and the initial crack length a_0

$$E_f = \frac{3a_0^3 + 2L^3}{8Bh^3}\left(C_0 - \frac{3L}{10G_{13}Bh}\right)^{-1} \qquad 10.15$$

This procedure takes into account the variableness of the material properties between different specimens and several effects that are not included in beam theory, e.g., stress concentration near the crack tip and contact between the two arms. In fact, these phenomena affect the specimen behavior and consequently the P-δ curve, even in the elastic regime. Using this methodology their influence are accounted for through the calculated flexural modulus. On the other hand, it is known that, during propagation, there is a region ahead of crack tip (Fracture Process Zone), where materials undergo properties degradation by different ways, e.g., micro-cracking, fibre bridging and inelastic processes. These phenomena affect the material compliance and should be accounted for in the mode II tests. Consequently, during crack propagation a correction of the real crack length is considered in the equation of compliance (10.14) to include the FPZ effect

$$C = \frac{3(a + \Delta a_{\mathrm{FPZ}})^3 + 2L^3}{8E_f Bh^3} + \frac{3L}{10G_{13}Bh} \qquad 10.16$$

and consequently,

$$a_{\mathrm{eq}} = a + \Delta a_{\mathrm{FPZ}} = \left[\frac{C_{\mathrm{corr}}}{C_{0\,\mathrm{corr}}} a_0^3 + \frac{2}{3}\left(\frac{C_{\mathrm{corr}}}{C_{0\,\mathrm{corr}}} - 1\right)L^3\right]^{1/3} \qquad 10.17$$

where C_{corr} is given by

$$C_{\mathrm{corr}} = C - \frac{3L}{10G_{13}Bh} \qquad 10.18$$

G_{IIc} can now be obtained from

$$G_{\mathrm{IIc}} = \frac{9P^2 a_{\mathrm{eq}}^2}{16B^2 E_f h^3} \qquad 10.19$$

This data reduction scheme presents several advantages. Using this methodology crack measurements are unnecessary. Experimentally, it is only necessary to register the values of applied load and displacement. Therefore, the method is designated as Compliance-Based Beam Method (CBBM). Using this procedure the FPZ effects, that are pronounced in mode II tests, are included on the toughness measurement. Moreover, the flexural modulus is calculated from the initial compliance and initial crack length, thus avoiding the influence of specimen variability on the results. The unique material property needed in this approach is G_{13}. However, its effect on the measured G_{IIc} was verified to be negligible (de Moura *et al.*, 2006), which means that a typical value can be used rendering unnecessary to measure it.

ELS test

Following a procedure similar to the one described for the ENF test, the applied P-δ relationship is

$$\delta = \frac{dU}{dP} = \frac{P(3a^3 + L^3)}{2Bh^3E_1} + \frac{3PL}{5BhG_{13}} \qquad 10.20$$

In order to include the root rotation effects at clamping and the details of crack tip stresses or strains not included in the beam theory, an effective beam length (L_{ef}) can be achieved. In fact, considering in Equation 10.20 the initial crack length (a_0) and the initial compliance (C_0) experimentally measured, it can be written

$$C_0 - \frac{3a_0^3}{2Bh^3E_1} = \frac{L_{\text{ef}}^3}{2Bh^3E_1} + \frac{3L_{\text{ef}}}{5BhG_{13}} \qquad 10.21$$

To take account for the FPZ influence a correction to the real crack length (Δa_{FPZ}) should be considered. From Equation 10.20 the compliance (C) during crack propagation can be expressed as

$$C - \frac{3(a + \Delta a_{\text{FPZ}})^3}{2Bh^3E_1} = \frac{L_{\text{ef}}^3}{2Bh^3E_1} + \frac{3L_{\text{ef}}}{5BhG_{13}} \qquad 10.22$$

Combining Equations 10.22 and 10.21, the equivalent crack length can be given by

$$a_{\text{eq}} = a + \Delta a_{\text{FPZ}} = \left[(C - C_0)\frac{2Bh^3E_1}{3} + a_0^3\right]^{1/3} \qquad 10.23$$

G_{IIc} can now be obtained from

$$G_{\text{IIc}} = \frac{9P^2a_{\text{eq}}^2}{4B^2h^3E_1} \qquad 10.24$$

Following this procedure G_{IIc} can be obtained without crack measurement during propagation which can be considered an important advantage. Equation 10.24 only depends on applied load and displacement during crack growth. Additionally, the influence of root rotation at the clamping point and singularity effects at the crack tip are accounted for, through initial compliance C_0. During propagation, the effect of FPZ on the compliance is also included using this methodology. In this case (ELS test) it is necessary to measure the longitudinal modulus.

10.2.3 Numerical simulations

In order to verify the performance of the CBBM on the determination of G_{IIc} of unidirectional composites, numerical simulations of the ENF and ELS tests were performed. A cohesive mixed-mode damage model based on interface finite elements was considered to simulate damage initiation and propagation. A constitutive relation between the vectors of stresses (σ) and relative displacements (δ) is postulated (Fig. 10.2). The method requires local strengths ($\sigma_{u,i}$, i = I, II, III) and the critical strain energy release rates (G_{ic}) as inputted data parameters [8, 9]. Damage onset is predicted using a quadratic stress criterion

$$\begin{aligned} &\left(\frac{\sigma_{I}}{\sigma_{u,I}}\right)^2 + \left(\frac{\sigma_{II}}{\sigma_{u,II}}\right)^2 + \left(\frac{\sigma_{III}}{\sigma_{u,III}}\right)^2 = 1 \quad \text{if } \sigma_I \geq 0 \\ &\left(\frac{\sigma_{II}}{\sigma_{u,II}}\right)^2 + \left(\frac{\sigma_{III}}{\sigma_{u,III}}\right)^2 = 1 \quad \text{if } \sigma_I \leq 0 \end{aligned} \qquad 10.25$$

where σ_i, (i = I, II, III) represent the stresses in each mode. Crack propagation was simulated by a linear energy criterion

$$\frac{G_I}{G_{Ic}} + \frac{G_{II}}{G_{IIc}} + \frac{G_{III}}{G_{IIIc}} = 1 \qquad 10.26$$

Basically, it is assumed that the area under the minor triangle of Fig. 10.2 is the energy released in each mode, which is compared to the respective critical fracture energy represented by the bigger triangle. The subscripts *o* and *u* refer to the onset and ultimate relative displacement and the subscript *m* applies to the mixed-mode case. More details about this model are presented in de Moura *et al*. (2006).

Three-dimensional approaches (Figs 10.3 and 10.4) were carried out to include all the effects that can influence the measured G_{IIc}. The interface elements were placed at the mid-plane of the specimens to simulate damage progression. Very refined meshes were considered in the region of interest corresponding to crack initiation and growth. The specimens' geometry and

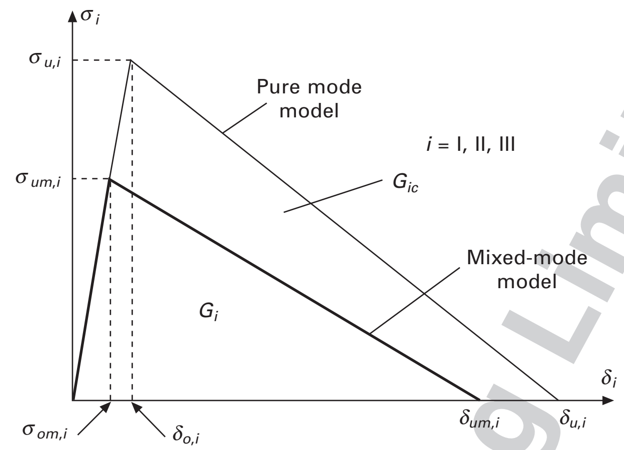

10.2 Pure and mixed-mode damage model.

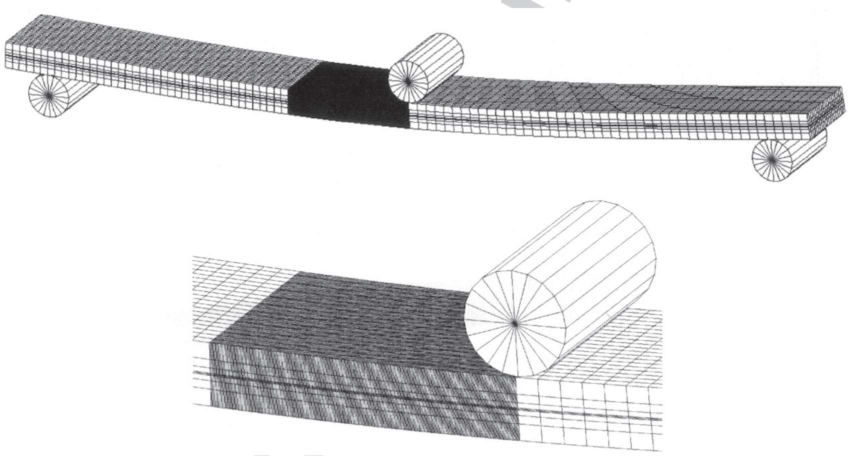

10.3 The mesh used for the ENF test: global view and detail of the refined mesh at the region of crack initiation and growth.

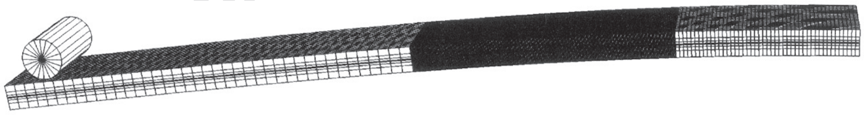

10.4 The mesh used for the ELS test.

material properties and are listed in Tables 10.1, 10.2 and 10.3, respectively. An analysis of *G*'s distributions at the crack front showed a clear predominance of mode II along the specimens' width, although some spurious mode III exists at the specimens edges (de Moura *et al*., 2006 and Silva *et al*., 2007).

Table 10.1 Specimens' geometry

	L (mm)	b (mm)	h (mm)	a_0 (mm)
ENF	100	10	1.5	75
ELS	100	10	1.5	60

Table 10.2 Material properties

E_1 (GPa)	$E_2 = E_3$ (GPa)	$\nu_{12} = \nu_{13}$	ν_{23}	$G_{12} = G_{13}$ (GPa)	G_{23} (GPa)
150	11	0.25	0.4	6	3.9

Table 10.3 Strength properties

$\sigma_{u,i}$ (i = I,II,III) (MPa)	G_{Ic} (N/mm)	G_{IIc} (N/mm)	G_{IIIc} (N/mm)
40	0.3	0.7	1.0

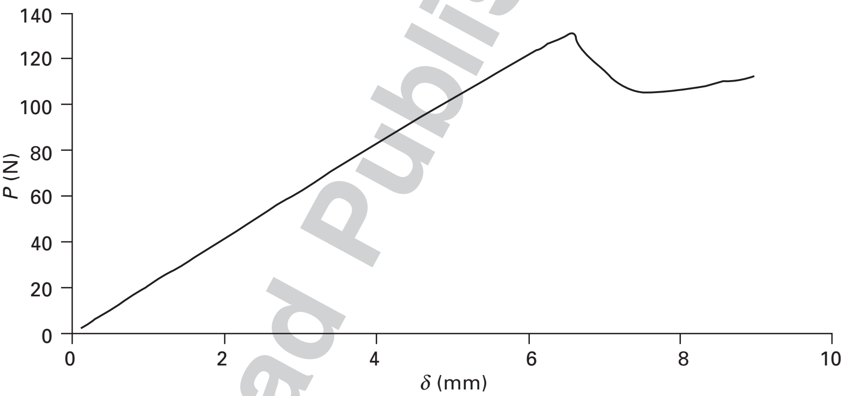

10.5 P-δ curve of the ENF specimen.

Appropriate values of critical strain energy release rates were considered for each of the three modes, respectively (see Table 10.3). Consequently, the efficacy of the proposed data reduction scheme can be evaluated by its capacity to reproduce the inputted G_{IIc} from the P-δ results obtained numerically.

The application of the CBBM is performed by three main steps. The first one is the measurement of the initial compliance C_0 from the initial slope of the P-δ curves (Figs (10.5) or (10.7)). This parameter is then used to estimate the flexural modulus in the ENF test (Equation 10.15). The next step is the evaluation of the equivalent crack length (Equations 10.17 or 10.23) in function of the current (C) and initial compliance (C_0). Finally, the R-curves, Figs (10.6) and (10.8), can be obtained from Equations 10.19 and 10.24, respectively. It should be noted that crack propagation occurs after peak load in both tests. During crack growth P decreases with the increase of equivalent crack length. This originates a plateau on the R-curves, which corresponds to the critical strain energy release rate in mode II (G_{IIc}). These plateau values are compared with the reference value (Figs (10.6) and (10.8)), which represents the inputted G_{IIc}. The excellent agreement obtained in both cases demonstrates the

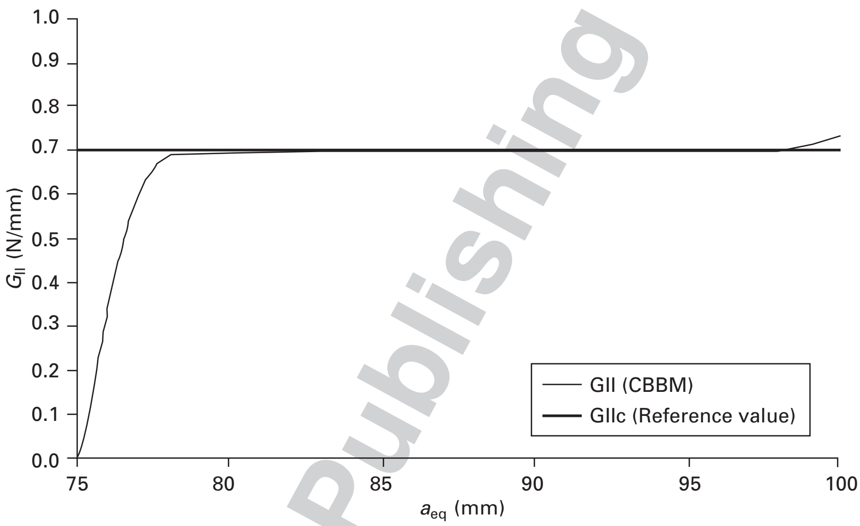

10.6 R-curve of the ENF specimen.

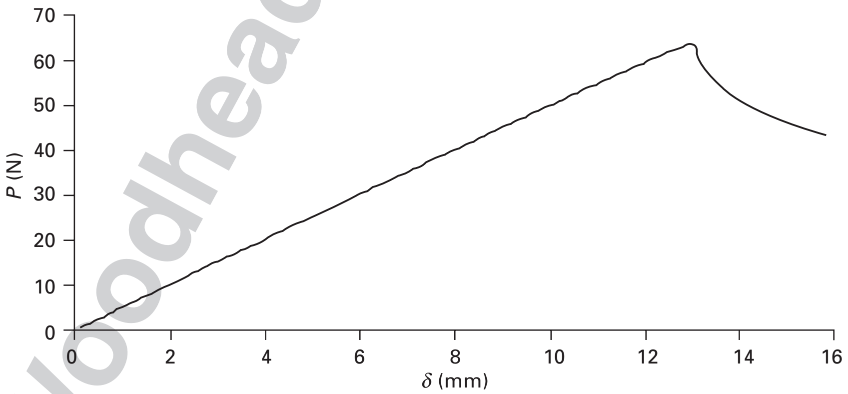

10.7 P-δ curve of the ELS specimen.

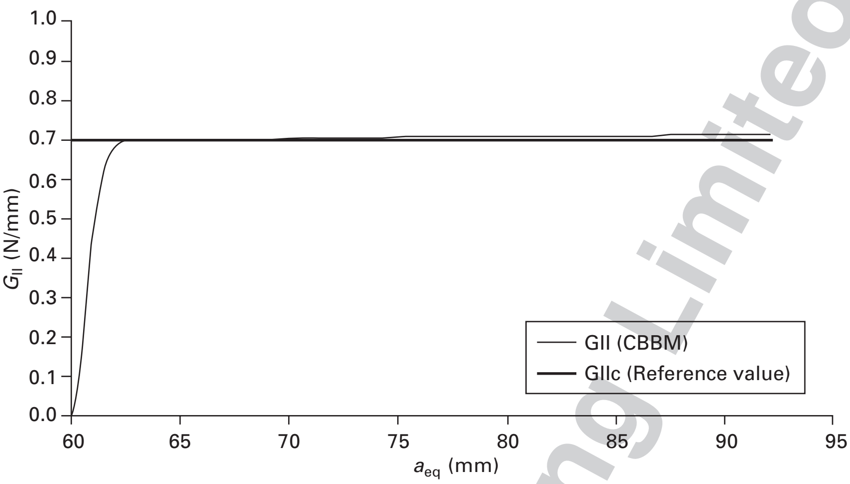

10.8 R-curve of the ELS specimen.

effectiveness of the CBBM as a suitable data reduction scheme to determine G_{IIc}, without crack length monitoring during propagation. As the ENF test is much simpler to execute than the ELS one, it can be concluded that using the CBBM, the ENF test is the most suitable for the determination of G_{IIc} and it should be considered as the principal candidate for standardization.

10.3 Dynamic mode II fracture characterization

The research on dynamic crack propagation in composites has become the focus of several authors in the recent years. The dynamic fracture characterization of composites is not easy to perform. In fact, it is experimentally difficult to induce high speed delamination growth in a simple and controlled manner (Guo and Sun, 1998). However, the determination of dynamic fracture toughness of composites is of fundamental importance in the prediction of the dynamic delamination propagation in composite structures. In addition, it is known that the impact delamination is mainly governed by mode II fracture (Wang and Vu-Khanh, 1991). However, there are several unclear phenomena related to dynamic crack propagation. One of the most important issues is related to the influence of rate effects on the propagation of dynamic cracks. An example of this occurrence is the dynamic delamination propagation occurring in composites submitted to low velocity impact. In this case, rate effects in the FPZ can interact with the well known rate-dependency of polymers leading to a very complicated phenomenon. In addition, Kumar and Narayanan (1993) verified that when glass fibre reinforced epoxy laminates are impacted, the total delamination area between the various plies multiplied by the quasi-static energy release rate exceeds the energy of the impacting mass. This suggests that under high crack speeds, delamination propagates at lower toughness which leads to larger damaged areas. In order to explain this behaviour, Maikuma *et al*. (1990) suggest that the calculation of critical strain energy release rate should account for the kinetic energy (E_{kin}) in Equation 10.26

$$G_{IIc} = \frac{P^2}{2B}\frac{dC}{da} - \frac{dE_{kin}}{B\,da} \qquad 10.27$$

The kinetic energy expression can be obtained from

$$E_{kin} = \frac{1}{2}\rho B 2h \int_0^{L_t} \left(\frac{dw(x)}{dt}\right)^2 dx \qquad 10.28$$

where ρ and L_t are the mass density and the total length of the specimen, respectively, t represents the time and $w(x)$ the displacement field. The quasi-static approach may provide an adequate approximation to the dynamic problem if the contribution of kinetic energy is small.

Wang and Vu-Khanh (1995) have suggested that the dynamic fracture behaviour of materials depends on the balance between the energy released by the structure over a unit area of crack propagation (G) and the material resistance (R), which can be viewed as the energy dissipated in creating the fracture surface. When unstable crack growth occurs, the difference G-R is converted into kinetic energy. If G increases with crack growth the crack speed also increases because more energy is available. Crack arrest will occur when G becomes lower than R and, consequently, no kinetic energy is available for crack growth. Thus, it can be affirmed that fracture stability depends on the variations of the strain energy release rate and the materials resistance during crack growth. On the other hand, the fracture resistance of polymer composites is generally sensitive to loading rate. Under impact load or during rapid delamination growth, the strain rate at the crack tip can be very high and the material toughness significantly reduced. The fracture surface exhibited ductile tearing and large scale plastic deformation of the matrix. The dynamic fracture surface in the initiation exhibits less plastic deformation; during propagation even less deformation is observed. It was also verified that plastic zone size at the crack tip diminishes with increasing rate. Consequently, the decrease in mode II interlaminar fracture toughness is attributed to a transition from ductile to brittle matrix dominated failure with increasing rate.

The decreasing trend of toughness with increase of crack speed was also observed by Kumar and Kishore (1998). The authors used a combination of numerical and experimental techniques on the DCB specimens to carry out dynamic interlaminar toughness measurements of unidirectional glass fibre epoxy laminate. They observed a sharp decrease of dynamic toughness values relatively to the quasi-static ones. In fact, they measured dynamic toughness initiation values of 90–230 N/m^2 against quasi-static values of 344–478 N/m^2. Propagation values of 0–50 N/m^2 were obtained for crack speed ranging between 622–1016 m/s.

The majority of the experimental studies consider unidirectional laminates. Lambros and Rosakis (1997) performed an experimental investigation of dynamic crack initiation and growth in unidirectional fibre-reinforced polymeric-matrix thick composite plates. Edge-notched plates were impacted in a one-point bend configuration using a drop-weight tower. Using an optical method the authors carried out a real-time visualization of dynamic fracture initiation and growth for crack speeds up to 900 m/s. They verified that the elastic constants of the used material are rate sensitive and the measured fracture toughness values are close to those typical of epoxies. This was considered consistent, because in unidirectional lay-ups crack initiation and growth occurs in the matrix.

Tsai *et al*. (2001) used a modified ENF specimen to determine the mode II dominated dynamic delamination fracture toughness of fiber composites at high crack propagation speeds. A strip of adhesive film with higher toughness was placed at the tip of interlaminar crack created during laminate lay-up. The objective was to delay the onset of crack extension and produce crack propagation at high speeds (700 m/s). Sixteen pure aluminium conductive lines were put on the specimen edge side using the vapour deposition technique, to carry out crack speed measurements. The authors concluded that the mode II dynamic energy release rate of unidirectional S2/8553 glass/epoxy composite seems to be insensitive to crack speed within the range of 350 and 700 m/s. The authors also simulated mixed mode crack propagation by moving the pre-crack from the mid-plane to 1/3 of the ENF specimen thickness of unidirectional AS4/3501-6 carbon/epoxy laminates. The maximum induced crack speed produced was 1100 m/s. They found that that the critical dynamic energy release rate is not affected by the crack speed and lies within the scatter range of the respective static values.

For numerical simulations of the dynamic crack propagation the cohesive damage models emerge as the most promising tools. The major difficulty is the incorporation of the rate-dependent effects in the constitutive laws. Corigliano *et al*. (2003) developed a cohesive crack model with a rate-dependent exponential interface law to simulate the nucleation and propagation of cracks subjected to mode I dynamic loading. The model is able to simulate the rate-dependent effects on the dynamic debonding process in composites. The authors concluded that the softening process occurs under larger relative displacements in comparison to rate-independent models. They verified that the type of rate-dependency can affect dynamic crack processes, namely the time to rupture and fracture energy. They also state that these effects diminish when inertial terms become dominant.

In summary, dynamic fracture toughness characterization of composite materials has been the centre of attention of several authors with no apparent consensus on the results. Although the majority of the studies point to a decrease of the fracture toughness with increasing load rate there is no unanimity about this topic. Some authors observed the opposite trend (Corigliano *et al*., 2003) and others detected no remarkable influence of crack speed on toughness (Tsai *et al*., 2001). Although some of these discrepancies can eventually be explained by different behaviour of the tested materials, and the attained crack speed values, it is obvious that more profound studies about the subject are necessary.

10.4 Conclusions

Interlaminar fracture characterization of composites in mode II acquires special relevancy namely under transverse loading such as low velocity impact. Up to now there is no standardized test in order to measure the critical strain energy release rate in mode II. Due to their simplicity, the ENF and ELS tests become the principal candidates to standardization. However, they present a common difficulty associated with crack monitoring during propagation which is fundamental to obtaining the *R*-curves, following the classical data reduction schemes. To surmount these difficulties a new data reduction scheme based on specimen compliance is proposed. The method does not require crack length measurement during propagation, and accounts for the effects of the quite extensive FPZ on the measured critical strain energy release rate. Numerical simulations of the ENF and ELS tests demonstrated the adequacy and suitability of the proposed method to obtain the mode II *R*-curves of composites. Due to its simplicity the ENF test is proposed for standardization.

Little work has been done on dynamic fracture of composite materials, namely under mode II loading. This is due to experimental difficulties related to inducing high crack speeds in a monitored way. Although the majority of the published works point to a decrease of the dynamic toughness with increase of crack speed, it appears that dynamic toughness can be similar to the respective quasi-static value up to a given crack speed (Tsai *et al*., 2001). Undoubtedly, more research about this topic is necessary. In fact, an unsafe structural design can occur if the quasi-static values of toughness are used in a dynamically loaded structure.

10.5 Acknowledgements

The author thanks Professors Alfredo B. de Morais (UA, Portugal), José Morais (UTAD, Portugal) and Manuel Silva for their valorous collaboration, advices and discussion about the matters included in this chapter. The author also thanks the Portuguese Foundation for Science and Technology for supporting part of the work here presented, through the research project POCI/EME/56567/2004.

10.6 References

Barrett JD, Foschi RO (1977), 'Mode II stress-intensity factors for cracked wood beams', *Engng. Fract. Mech.*, 9: 371–378.

Carlsson LA, Gillespie JW, Pipes RB (1986), 'On the analysis and design of the end notched flexure (ENF) specimen for mode II testing', *J Compos Mater*, 20: 594–604.

Choi HY, Chang FK (1992), 'A model for predicting damage in graphite/epoxy laminated composites resulting from low-velocity point impact', *J Compos Mater*, 26: 2134–2169.

Corigliano A, Mariani S, Pandolfi A (2003), 'Numerical modelling of rate-dependent debonding processes in composites', *Compos. Struct.*, 61: 39–50.

Davidson BD, Sun X (2005), 'Effects of friction, geometry and fixture compliance on the perceived compliance from three- and four-point bend end-notched flexure tests', *J. Reinf. Plastics Compos.*, 24: 1611–1628.

Davies P, Blackman BRK, Brunner AJ (2001), Mode II delamination. In: Moore DR, Pavan A, Williams JG, editors. *Fracture Mechanics Testing Methods for Polymers Adhesives and Composites*, Amsterdam, London, New York: Elsevier; 307–334.

de Morais AB, Pereira AB (2007), 'Application of the effective crack method to mode I and mode II interlaminar fracture of carbon/epoxy unidirectional laminates', *Composites Part A: Applied Science and Manufacturing*, 38: 785–794.

de Moura MFSF, Silva MAL, de Morais AB, Morais JJL (2006), 'Equivalent crack based mode II fracture characterization of wood', *Engng. Fract. Mech.*, 73: 978–993.

Guo C, Sun CT (1998), 'Dynamic mode-I crack propagation in a carbon/epoxy composite', *Composites Science and Technology*, 58: 1405–1410.

Kageyama K, Kikuchi M, Yanagisawa N (1991), 'Stabilized end notched flexure test: characterization of mode II interlaminar crack growth'. In: O'Brien TK, editor. *Composite Materials: Fatigue and Fracture*, ASTM STP 1110, Vol. 3. Philadelphia PA: ASTM, p. 210–225.

Kanninen MF, Popelar CH (1985), *Advanced Fracture Mechanics*, Oxford: Oxford University Press.

Kumar P, Narayanan MD (1993), 'Energy dissipation of projectile impacted panels of glass fabric reinforced composites', *Compos. Struct.*, 15: 75–90.

Kumar P, Kishore NN (1998), 'Initiation and propagation toughness of delamination crack uncder an impact load', *J. Mech. Phys. Solids*, 46: 1773–1787.

Lambros J, Rosakis AJ (1997), 'Dynamic crack initiation and growth in thick unidirectional graphite/epoxy plates', *Composites Science & Technology*, 57: 55–65.

Maikuma H, Gillespie JW, Wilkins DJ (1990), 'Mode II interlaminar fracture of the center notch flexural specimen under impact loading', *J. Compos. Mater.*, 24: 124–149.

Schuecker C, Davidson BD (2000), 'Effect of friction on the perceived mode II delamination toughness from three and four point bend end notched flexure tests', ASTM STP, 1383: 334–344.

Silva MAL (2006), 'Estudo das Propriedades de Fractura em Modo II e em Modo III da Madeira de Pinus pinaster Ait.', Master Thesis, FEUP, Porto.

Silva MAL, Morais JJL, de Moura MFSF, Lousada JL (2007), 'Mode II wood fracture characterization using the ELS test', *Eng. Fract. Mech.*, 74: 2133–2147.
Tanaka K, Kageyama K, Hojo M (1995), 'Prestandardization study on mode II interlaminar fracture toughness test for CFRP in Japan', *Composites*, 26: 243–255.
Tsai JL, Guo C, Sun CT (2001), 'Dynamic delamination fracture toughness in unidirectional polymeric composites', *Composites Science & Technology*, 61: 87–94.
Yoshihara H, Ohta M (2000), 'Measurement of mode II fracture toughness of wood by the end-notched flexure test, *J Wood Sci*., 46: 273–278.
Yoshihara H (2004), 'Mode II *R*-curve of wood measured by 4-ENF test', *Engng. Fract. Mech*., 71: 2065–2077.
Wang H, Vu-Khanh T (1991), 'Impact-induced delamination in [05, 905, 05] carbon fiber/Polyetheretherketone composite laminates', *Polymer Engineering and Science*, 31: 1301–1309.
Wang H, Vu-Khanh T (1995), 'Fracture mechanics and mechanisms of impact-induced delamination in laminated composites', *J. Compos. Mater.*, 29: 156–178.
Wang H, Vu-Khanh T (1996), 'Use of end-loaded-split (ELS) test to study stable fracture behaviour of composites under mode II loading', *Compos. Struct*., 36: 71–79.
Wang Y, Williams JG (1992), 'Corrections for Mode II Fracture Toughness Specimens of Composite Materials', *Composites Science & Technology*, 43: 251–256.